Development 140, 1912-1918 (2013) doi:10.1242/dev.093583

Ssrp1a controls organogenesis by promoting cell cycle progression and RNA synthesis

Katarzyna Koltowska[1,*], Holger Apitz[2], Despina Stamataki[1], Elizabeth M. A. Hirst[3], Heather Verkade[4], Iris Salecker[2] and Elke A. Ober[1,‡]

SUMMARY

Tightly controlled DNA replication and RNA transcription are essential for differentiation and tissue growth in multicellular organisms. Histone chaperones, including the FACT (facilitates chromatin transcription) complex, are central for these processes and act by mediating DNA access through nucleosome reorganisation. However, their roles in vertebrate organogenesis are poorly understood. Here, we report the identification of zebrafish mutants for the gene encoding Structure specific recognition protein 1a (Ssrp1a), which, together with Spt16, forms the FACT heterodimer. Focussing on the liver and eye, we show that zygotic Ssrp1a is essential for proliferation and differentiation during organogenesis. Specifically, gene expression indicative of progressive organ differentiation is disrupted and RNA transcription is globally reduced. Ssrp1a-deficient embryos exhibit DNA synthesis defects and prolonged S phase, uncovering a role distinct from that of Spt16, which promotes G_1 phase progression. Gene deletion/replacement experiments in *Drosophila* show that Ssrp1b, Ssrp1a and N-terminal Ssrp1a, equivalent to the yeast homologue Pob3, can substitute *Drosophila* Ssrp function. These data suggest that (1) Ssrp1b does not compensate for Ssrp1a loss in the zebrafish embryo, probably owing to insufficient expression levels, and (2) despite fundamental structural differences, the mechanisms mediating DNA accessibility by FACT are conserved between yeast and metazoans. We propose that the essential functions of Ssrp1a in DNA replication and gene transcription, together with its dynamic spatiotemporal expression, ensure organ-specific differentiation and proportional growth, which are crucial for the forming embryo.

KEY WORDS: Ssrp1, Cell cycle, Hdac, Liver, Organogenesis, Zebrafish, *Drosophila*

INTRODUCTION

Expansion of progenitor pools and their tissue-specific differentiation are central for the formation of functional organs. Complex signalling cascades controlling organ growth and differentiation have been identified, but the associated basic cellular processes, such as regulation of DNA accessibility, in the developing embryo are still poorly understood. DNA accessibility, allowing the passage of RNA polymerase II and replication forks, is pivotal for coordinated gene expression and cell proliferation. Histone chaperones mediate DNA accessibility by structural destabilisation of nucleosomes and deconvolution of higher-order chromatin structure (Ransom et al., 2010). One histone chaperone, the FACT (facilitates chromatin transcription) complex consists of Spt16 (suppressor of Ty16; also known as Supt16h in zebrafish) and Ssrp1 (Structure specific recognition protein 1), which are both essential for nucleosome reorganisation and conserved across metazoans and plants (Formosa, 2008; Winkler and Luger, 2011). Metazoan Ssrp1 contains a C-terminal high mobility group box (HMGB), whereas its yeast homologue Pob3 solely encodes the N-terminal domains and the HMGB function is provided by the small independent protein Nhp6 (Brewster et al., 2001; Formosa et al., 2001; Stillman, 2010). Both yeast Spt16 and Pob3 are required for cell viability, whereas Nhp6 is not essential (Malone et al., 1991; Wittmeyer et al., 1999; Brewster et al., 2001), questioning the importance of the HMGB domain of Ssrp1 for FACT function in metazoans. In mice, Ssrp1 loss results in lethality around implantation (Cao et al., 2003). Consequently, insights into Ssrp1 and FACT functions during later stages of vertebrate embryogenesis are limited.

Here, we report that the FACT component Ssrp1a is essential for tissue differentiation and growth in vertebrate organogenesis. In the developing zebrafish liver and eye, zygotic loss of Ssrp1a results in impaired RNA transcription, defective S phase progression and cell death. Using cross-species rescue experiments, we examine the importance of the HMGB domain of Ssrp1a, as well as paralogous Ssrp1b, in metazoan organogenesis.

MATERIALS AND METHODS

Fish stocks

The following strains were bred under standard conditions (Westerfield, 2000): *Tg(XIEef1a1:GFP)^{s854}* (Field et al., 2003), *clamped^{s819}*, *clamped^{u428}*, *cecyil: Tg(Efα:mKO2-zCdt1(1/190))^{rw0405b}; Tg(Efα:mAG-zGem(1/100))^{rw0410h}* (Sugiyama et al., 2009) and *tp53^{zdf1}* (Berghmans et al., 2005) (for genotyping details, see Zebrafish International Resource Center).

Positional cloning of *clamped^{s819}*

Meiotic mapping followed standard protocols (Geisler, 2002). Sibling and *cmp^{s819}* mutant cDNAs were sequenced for *ssrp1a*, *rad9a*, *zgc:113229*, *med19a* and *slc43a1a*. For genotyping of homozygous *cmp^{s819}* embryos, dCaps Finder 2.0 (http://helix.wustl.edu/dcaps/dcaps.html) was used to design primers creating a *Hin*fI restriction site including the *ssrp1a^{s819}* mutation. The following primers were used for PCR amplification from genomic DNA: forward 5′-AGCTCATTAGCACACAGATGG-3′ and reverse 5′-CAGTTCCCCAATTCCAGCCCTTGAC-3′. PCR amplification and subsequent *Hin*fI digest from homozygous mutant, wild-type and heterozygous embryos confirmed the identified lesion (supplementary material Fig. S1). ‘MO-ssrp1a’ (MO-ATG-ssrp1a, 5′-CGTTAAACT-CCAGAGTGTCTCCCAT-3′; Gene Tools) and standard ‘MO-control’ were injected into one-cell-stage wild-type or *Tg(XIEef1a1:GFP)^{s854}* zebrafish.

Divisions of [1]Developmental Biology, [2]Molecular Neurobiology and [3]Developmental Neurobiology, MRC National Institute for Medical Research, London, NW7 1AA, UK. [4]School of Biological Sciences, Monash University, Clayton VIC 3800, Australia.

*Present address: Institute for Molecular Biosciences, University of Queensland, St Lucia, Queensland 4072, Australia
‡Author for correspondence (eober@nimr.mrc.ac.uk)

Accepted 22 February 2013

Zebrafish immunostaining and *in situ* hybridisation

Labelling was performed as described (Ober et al., 2006). The following antibodies were used: rabbit anti-Prox1 (1:1000; Chemicon), mouse anti-2F11 (1:1000; gift from J. Lewis, Cancer Research UK, London, UK), mouse anti-BrdU [1:20; Developmental Studies Hybridoma Bank (DSHB)] and rabbit anti-cleaved Caspase 3 (1:75; Cell Signaling Technology). Fluorescently conjugated secondary antibodies were obtained from Jackson Laboratories. Staining was visualised with a Zeiss LSM5Pascal Exciter confocal microscope. Images were processed and cell numbers determined with Volocity image analysis software (Improvision).

The following probes were used for *in situ* hybridisation: *ath5* (also known as *atoh7*) (Masai et al., 2000), *ceruloplasmin* (Korzh et al., 2001), *ccne* (Shkumatava et al., 2004), *foxa1* (Odenthal and Nüsslein-Volhard, 1998), *group specific component* (Noël et al., 2010), *mdm2* (Chen et al., 2005), *p21* [*cyclin-dependent kinase inhibitor 1a* (*cdkn1a*)] (Chen et al., 2005), *pcna* (Leung et al., 2005) and *ptf1* (Lin et al., 2004).

BrdU incorporation assay

Embryos were incubated for 30 minutes at 28.5°C in 10 mM 5-bromo-deoxyuridine (BrdU) with 15% DMSO in embryo medium (5 mM NaCl, 0.17 mM KCl, 0.33 mM $CaCl_2$, 0.33 mM $MgSO_4$) and prior to immunolabelling were treated with 2 M HCl for one hour at room temperature.

Global RNA labelling

Embryos were incubated in 10 mM 5-ethynyluridine (EU; Invitrogen) with 15% DMSO in embryo medium for one hour at 28.5°C. Click-iT detection was performed following manufacturer's instructions (Invitrogen).

Mitotic index analysis

Foregut-containing tissue was isolated manually in Hank's balanced salt solution with 5% fetal calf serum on ice and passaged through a 40 μm filter. Single-cell suspensions were stained with Vybrant DyeCycle Ruby (Invitrogen) and analysed by fluorescence-activated cells sorting (FACS) (Calibur, Becton Dickinson). Raw data were analysed by FlowJo software.

Drosophila molecular biology, genetics and histology

Zebrafish genes were cloned into a modified pKC26 *UAS* vector containing an *attB* site and a 3′ V5 epitope-tag sequence. Plasmids were inserted into the *attP* site-containing locus VIE-260b to generate transgenic lines (for details, see Hadjieconomou et al., 2011). Genetic crosses are summarised in supplementary material Table S2. Dissected tissues were processed as described (Hadjieconomou et al., 2011) and labelled using mouse mAb24B10 (1:75; DSHB), rat anti-Elav (1:50; DSHB), rabbit anti-PH3 (1:100; Millipore/Upstate), rabbit anti-aPKC ς (1:100; sc-216, Santa Cruz) and mouse anti-V5 (1:500; Invitrogen) and fluorescently labelled $F(ab')_2$ fragments from Jackson ImmunoResearch Laboratories as secondary antibodies. Images were collected with a Bio-Rad/Zeiss Radiance2100 or a Leica TCS SP5II confocal microscope. Samples for scanning electron microscopy were prepared using standard procedures (Cheyette et al., 1994) and imaged with a JEOL 35CF microscope.

qPCR

Quantitative PCR (qPCR) was performed using primer sets for *ssrp1a* and *ssrp1b* (ssrp1a1F 5′-CCTCATCCTCCTGTTCTCCAAA-3′, ssrp1aR 5′-TCTCCACCTCATCTTCGCTCAT-3′; ssrp1bF 5′-TCCGGCTCTCTC-TATGAGATGG-3′, ssrp1bR 5'-TGTGATCTTCCTGTTGACCAAGG-3′; rpl13F, 5′-TCTGGAGGACTGTAAGAGGTATGC-3′; rpl13R, 5′-AGAC-GCACAATCTTGAGAGCAG-3′). mRNA was extracted from five to ten embryos and processed. qPCR (60°C annealing temperature) was carried out using ABsolute SYBR Green Mix (Thermo) on the ABI Prism 7000 RTPCR Detection system. Expression values were normalized using rpl13 and compared using Student's *t*-test. Unless otherwise indicated, three independent experiments were assessed with three samples each.

RESULTS AND DISCUSSION

The *clamped*^{s819} mutation disrupts organ growth and differentiation

The *clamped*^{s819} (*cmp*^{s819}) mutant was previously identified in a forward genetic screen for factors essential for endodermal organogenesis (Ober et al., 2006). *cmp*^{s819} embryos display liver and pancreas hypoplasia at 48 hours post-fertilisation (hpf; Fig. 1A-D), and smaller fins, head and eyes from 40 hpf (Fig. 2B-E). Liver progenitors arise from the foregut endoderm and aggregate into the liver bud (Field et al., 2003). Concomitant with liver-bud outgrowth, hepatoblasts begin to differentiate into functional hepatocytes and biliary epithelial cells. From about 50 hpf, the liver grows rapidly. Quantification of hepatic progenitors in *cmp*^{s819} mutants using Prox1 expression showed a 40% reduction at 48 hpf (Fig. 1B-D). *ceruloplasmin* (*cp*), which encodes a plasma protein in differentiating hepatoblasts (Korzh et al., 2001), is expressed in *cmp*^{s819} mutant livers at 48 hpf, but is not maintained at 96 hpf (100%, *n*=18 and *n*=10, respectively; Fig. 1E-H). In addition, *group specific component* (*gc*), marking late hepatocyte differentiation (Noël et al., 2010), was not detected in *cmp*^{s819} mutants (100%, *n*=15; Fig. 1I-J). Hence, hepatic differentiation fails to progress in *cmp*^{s819} mutants. Moreover, pan-endodermal expression of the transcription factor *foxa1* in *cmp*^{s819} mutants is similar to wild type at 40 hpf (100%, *n*=12; Fig. 1K,L), but undetectable at 72 hpf (100%, *n*=9; Fig. 1M,N). This is due to defects in transcription and not tissue loss, as *Tg(XIEef1a1:GFP)*^{s854} labels the digestive system in controls and *cmp*^{s819} mutants at 72 hpf (100%, *n*=10; Fig. 1O,P). In wild-type embryos, EU labelling of newly synthesised RNA (Jao and Salic, 2008) was detected in all nuclei with higher levels in transcriptionally active sites at 48 hpf (Fig. 1Q-Q″). These foci were largely absent in *cmp*^{s819} mutants and overall EU incorporation levels were lower (Fig. 1R-R″), indicating a general defect in RNA transcription. Consistently, actively transcribed genes with a short mRNA half-life, such as those encoding cyclins (Ohtani et al., 1995), represent some of the first genes exhibiting mRNA transcription defects (supplementary material Fig. S4L,M). Altogether, this suggests that *cmp*^{s819} affects a key factor mediating gene transcription in the differentiating zebrafish liver.

clamped mutations disrupt an orthologue of Ssrp1

Meiotic recombination mapping placed the *cmp*^{s819} mutation on linkage group 14 in a 340-kb genomic region between markers *mindin1* (*spon2a*) and rs411174000 (primers amplifying a ~160 bp product in an intron of *ccng1*: F: 5′-GCATAAAACGTC-TCTGTGTGC-3′; R: 5′-GCAGAGAGGAGATGAGGAAAC-3′) (Fig. 2A). Sequencing of five candidate genes within this region revealed a T-to-A base pair substitution at position 309 of *ssrp1a* in *cmp*^{s819} mutants, resulting in a premature stop codon and, thus, a truncated protein of 102 amino acids (aa), terminating halfway in the N-terminal Spt16-dimerisation domain (Fig. 2A). The *cmp*^{s819} lesion was confirmed in mutants by a derived cleaved amplified polymorphic sequences (dCaps) assay (supplementary material Fig. S1A). Moreover, the mutant *u428* failed to complement *cmp*^{s819} and contained a T-to-G base pair substitution at aa 221 in *ssrp1a* (R. Young, H. Stickney, T. Hawkins, F. Cavodeassi, G. Gestri, S. Wilson and E.A.O., unpublished; Fig. 2A). Both *cmp* mutations are predicted to produce functionally inactive proteins, compromising FACT complex formation and function (Keller and Lu, 2002).

Knockdown of Ssrp1a by injection of morpholino antisense oligonucleotides (MOs) into *Tg(XIEef1a1:GFP)*^{s854} embryos phenocopied *cmp* mutants, with ~80% of embryos showing digestive system hypoplasia (*n*=9) and 90% displaying smaller eyes, head and fins (*n*=126; Fig. 2B-G). Consistent with the RNA transcription defects in *cmp* mutants, previous studies implicated Ssrp1 function in transcription (Orphanides et al., 1999; Belotserkovskaya et al., 2003; Saunders et al., 2003; Bai et al.,

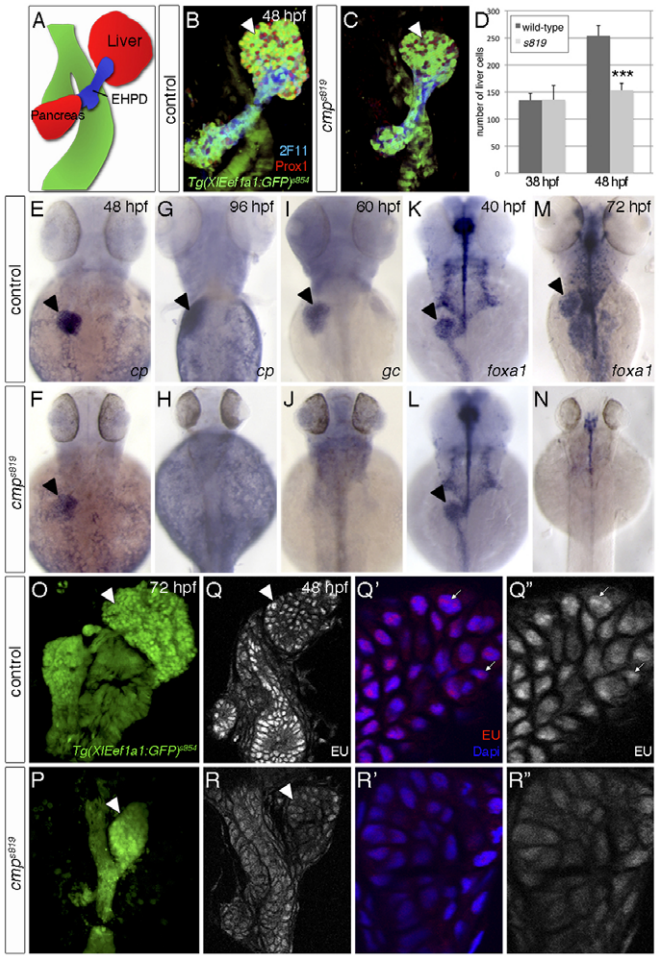

Fig. 1. *cmp*^{s819} controls endodermal differentiation and global transcription. (**A**) Schematic of endodermal organs. (**B**,**C**) Confocal projections of endodermal *Tg(XIEef1a1:GFP)*^{s854}, hepatic and pancreatic Prox1 and 2F11 in the extrahepatopancreatic ducts (EHPD) show liver and pancreas hypoplasia in *cmp*^{s819} mutants. (**D**) Prox1-positive hepatoblasts are significantly reduced in *cmp*^{s819} embryos at 48 hpf; data show mean±s.e.m., ***P=1.2^{-5}. (**E-H**) At 48 hpf, *cp* is expressed in *cmp*^{s819} livers (E,F), but undetectable at 96 hpf (G,H). (**I**,**J**) *gc* expression is absent in *cmp*^{s819} embryos at 60 hpf. (**K-N**) *foxa1* is expressed throughout the *cmp*^{s819} endoderm at 40 hpf (K,L) and is absent at 72 hpf, whereas residual *foxa1* is detectable in neural tissues (M,N). (**O**,**P**) *Tg(XIEef1a1:GFP)*^{s854} labels the digestive system in sibling and *cmp*^{s819} embryos at 72 hpf. (**Q-R″**) EU incorporation reveals reduced RNA transcription in the digestive system of *cmp*^{s819} mutants at 48 hpf. Using the same confocal settings, magnifications of representative sections show fewer EU-positive foci (arrows) in *cmp*^{s819} livers compared with controls. A-C,O-R″ are ventral views; E-N are dorsal views; all show anterior to the top. Arrowheads indicate liver.

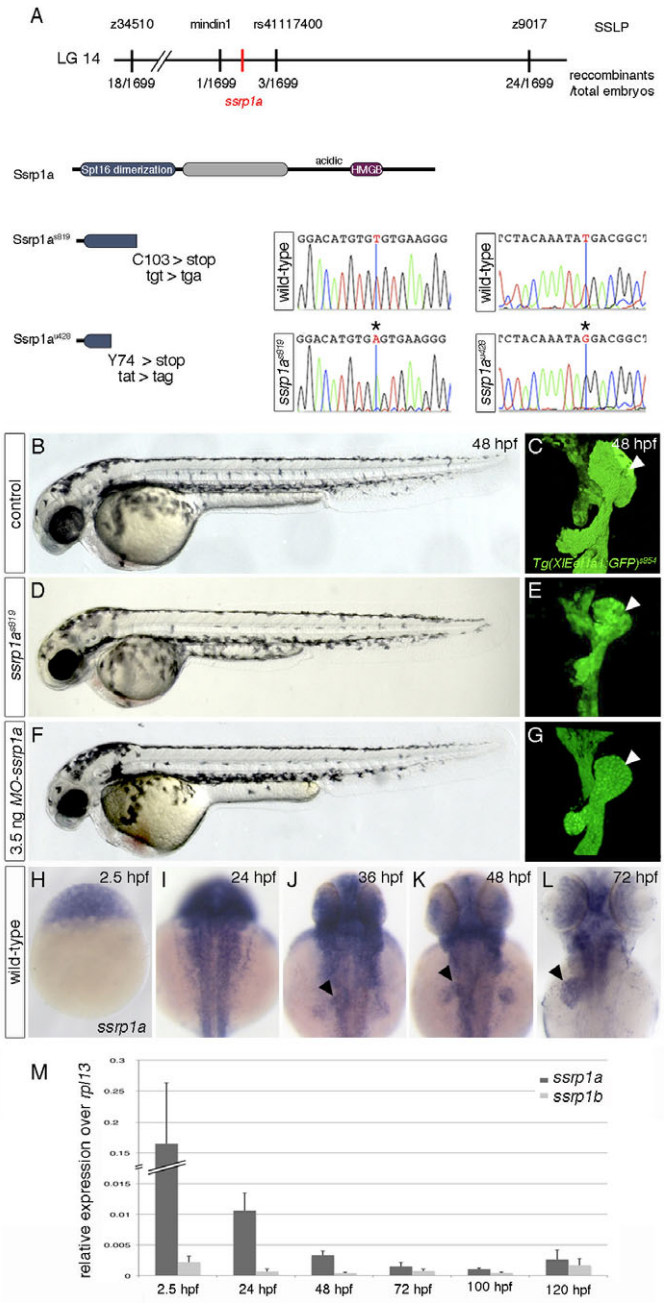

Fig. 2. *ssrp1a* is disrupted in *cmp* mutants. (**A**) Genetic map of the *cmp*-containing region. *s819*- and *u428*-lesions in *ssrp1a* are shown at the nucleotide and protein level. (**B-G**) *MO-ssrp1a*-injected embryos (F,G) phenocopy *cmp*^{s819} defects (D,E). Lateral views show smaller heads and eyes in mutant (D) and *MO-ssrp1a* embryos (F) compared with controls (B). Confocal projections of *Tg(XIEef1a1:GFP)*^{s854} highlight liver (arrowheads) and pancreas hypoplasia in *cmp*^{s819} (E), and *MO-ssrp1a* injected embryos (G) compared with controls (C); ventral views, anterior to the top. (**H-L**) *ssrp1a* expression in wild-type embryos between 2.5 and 72 hpf. Dorsal views, anterior to the top. After 24 hpf, *ssrp1a* is enriched in the liver (arrowheads), eyes and fins. (**M**) qPCR analyses show dynamic *ssrp1a* and *ssrp1b* expression levels between 2.5 and 120 hpf. Error bars represent s.d.

2010). Based on these validations, the *cmp* mutants are referred to as *ssrp1a*^{s819} and *ssrp1a*^{u428}. All experiments were performed with *ssrp1a*^{s819}, as both alleles display comparable phenotypes.

ssrp1a is expressed ubiquitously in the early embryo and from ~36 hpf in proliferative tissues, such as the liver, eyes and fins (Fig. 2H-L). Quantitative RT-PCR (qPCR) analysis revealed high maternal *ssrp1a* mRNA levels (2.5 hpf), whereas zygotic expression is much lower (>3 hpf; Fig. 2M). Inhibiting translation of maternal *ssrp1a* mRNA by MO injection into *Tg(XIEef1a1:GFP)*^{s854} embryos does not produce stronger phenotypes compared with *ssrp1a*^{s819} mutants (Fig. 2B-G), suggesting that maternal Ssrp1a protein compensates for Ssrp1a loss during early development. Alternatively, the zebrafish Ssrp1 paralogue Ssrp1b (81% identity)

might act redundantly (supplementary material Fig. S1B), as it is expressed throughout development, albeit at up to 98% lower levels than *ssrp1a* (Fig. 2M).

Ssrp1a promotes cell cycle progression in the digestive system and eye

Hepatic growth arrests in *ssrp1a*^{s819} mutants at ~48 hpf. BrdU incorporation experiments revealed that at 36 hpf proliferation rates in *ssrp1*^{s819} mutants (n=10) are similar to those in controls (n=13), but are reduced by ~10% at 38 hpf and by 87% at 49 hpf (n≥10; Fig. 3A-C). This indicates that Ssrp1a promotes hepatic cell divisions. To determine the Ssrp1a-dependent cell cycle phase, mutant and sibling livers were analysed in the transgenic *cecyil* background labelling S/G_2/M phase cells in green and G_1 phase cells in red (Sugiyama et al., 2009). At 38 hpf, 55-60% hepatoblasts are found in G_1 phase and ~40% in S/G_2/M phase in controls and *ssrp1a*^{s819} mutants (Fig. 3D,E,H). This distribution changes significantly in *ssrp1a*^{s819} mutants by 48 hpf, with 30% of cells in G_1 phase and 62% in S/G_2/M phase (n≥7; Fig. 3F-H), indicating that Ssrp1a-deficient hepatoblasts accumulate in S/G_2/M phase. Next, we examined single cell suspensions from the foregut domain of *Tg(XIEef1a1:GFP)*^{s854} embryos using FACS. Measuring the DNA content at 42-44 hpf revealed 18.5% fewer Ssrp1a-deficient endodermal cells in G_1 phase and, conversely, 10.5% more in S phase compared with wild type (Fig. 3I). This indicates that Ssrp1a is required for S phase progression during development, consistent with *in vitro* results reporting Ssrp1 functions in DNA elongation (Abe et al., 2011).

Our data indicate that Ssrp1a-deficient cells accumulate in S phase, probably owing to more cells entering or stalling in S phase. A role for Ssrp1a during DNA synthesis, rather than at subsequent checkpoints prior to mitosis, is corroborated by fewer cells incorporating BrdU, and the intact, not polyploid appearance of nuclei in *ssrp1a*^{s819} livers (Fig. 1Q′,R′). FACT interacts with the minichromosome maintenance (MCM) helicase in initiation and elongation of DNA synthesis (Gambus et al., 2006; Tan et al., 2006) and, consistent with this, cell cycle defects in *ssrp1a*^{s819} mutants resemble the ones in Mcm5-depleted zebrafish embryos (Ryu et al., 2005). Intriguingly, Spt16-depleted yeast exhibits a G_1 phase delay, pointing to specific functions of either FACT component (Morillo-Huesca et al., 2010). Similarly, human SSRP1 and SPT16 (SUPT16H) can regulate largely overlapping, but also distinct targets (Li et al., 2007).

To determine the specificity of different chromatin-remodelling factors on organ growth, we examined *hdac1*^{s436} mutants exhibiting similar liver size defects (Noël et al., 2008). Hdac1 mediates chromatin compaction and cell cycle progression from G_1 to S phase (Yamaguchi et al., 2010), raising the possibility that its loss might counterbalance *ssrp1a*^{s819} phenotypes. *cecyil*-based cell cycle analysis at 60 hpf showed that in *hdac1*^{s436} mutants 68% of cells are in G_1 phase and 15% in S/G_2/M phase (supplementary material Fig. S2A-E), suggesting that Hdac1 promotes cell cycle progression in liver organogenesis. Ssrp1a knockdown in *hdac1*^{s436} mutants partially rescues both individual phenotypes, with 26% cells in S/G_2/M phase and 55% in G_1 phase (supplementary material Fig. S2A-E), whereas neither organ size, nor hepatic gene expression improves (supplementary material Fig. S2F; data not shown). This is unexpected because in yeast impaired Ssrp1/Pob3 and Hdac/Rpd3(L) functions partially rescue gene transcription and cell viability compared with sole loss of Pob3 (Formosa et al., 2001). This suggests that both factors control different targets mediating cell viability in yeast and zebrafish liver growth.

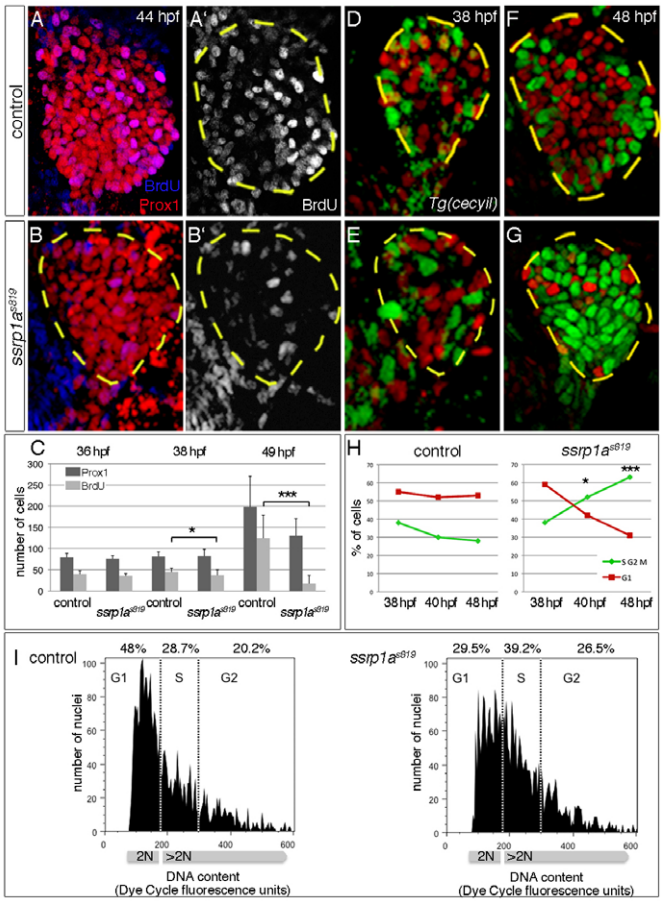

Fig. 3. Ssrp1a promotes cell cycle progression. (**A-C**) BrdU incorporation is reduced in *ssrp1a*^{s819} mutant livers from 38 hpf onwards (outlined). Error bars represent s.d. (**D-G**) Transgenic *cecyil* expression marks G_1 phase cells in red and S/G_2/M phase cells in green. (**H**) Quantification of hepatoblast proliferation shows a reversed distribution in controls and *ssrp1a*^{s819} mutants at 48 hpf. (**I**) FACS analysis of 42-44 hpf foregut endoderm shows an increase of cells in S phase and a decrease of those in G_1 phase in *ssrp1a*^{s819} mutants. A-B′,D-G are confocal projections of ventral views; all anterior to the top. *P<0.05, ***P<0.0005, determined by unpaired Student's t-test.

Compared with the liver, Ssrp1a is required earlier in retina differentiation and proliferation (~36 hpf; supplementary material Fig. S3), indicating similar, but temporally distinct, requirements for zygotic Ssrp1a in a tissue-specific manner. Liver and eye progenitors lacking Ssrp1a undergo apoptosis following S phase defects (supplementary material Fig. S3K-M and Fig. S4). Thus, in *ssrp1a*^{s819} mutants, incomplete DNA synthesis may trigger a DNA-damage response. Indeed, increased Tp53-target gene expression (Vogelstein et al., 2000) (supplementary material Fig. S4H-K) and a partial rescue of cell death in *ssrp1a;tp53* mutants (supplementary material Fig. S4F,G) showed that Tp53-dependent and -independent signalling is activated in Ssrp1a-deficient embryos. Human FACT activates TP53 following DNA damage (Keller et al., 2001) and in Ssrp1-deficient mice apoptosis is solely mediated by Tp53-independent pathways (Cao et al., 2003). By contrast, our data in zebrafish suggest that cell death is not mediated exclusively via Tp53, but might include alternative pathways, highlighting the complexity of the molecular mechanisms following replication stress in different vertebrates.

Full-length *ssrp1a* and *ssrp1b*, as well as *ssrp1a*$^{1-518}$, can compensate for the loss of *Drosophila Ssrp*

To elucidate the role of the HMGB domain, we performed cross-species rescue experiments using the *Drosophila* eye. The fly genome has one *Ssrp* gene (Shimojima et al., 2003), which encodes an HMGB-containing protein, similar to zebrafish Ssrp1a and Ssrp1b (supplementary material Fig. S1). Knockdown of Ssrp in the fly eye using a *UAS-Ssrp*^{RNAi} transgene caused severe defects (Fig. 4D-F″; supplementary material Fig. S6B,B′). Male pharate adults failed to eclose, and lacked eyes, antennae and head capsules, whereas 5.5% of females hatched, and displayed partial head capsules with absent or small eyes. Consistently, eye-antennal imaginal discs of third instar larvae were significantly smaller. Within the eye field, probably because of incomplete knockdown, few cells were phospho-Histone H3 (PH3) positive, and thus mitotically active, and few expressed Elav and mAb24B10 as indicators of photoreceptor (R-cell) differentiation. Upon overexpression of zebrafish full-length *ssrp1b*, full-length *ssrp1a*, *ssrp1a*^{s819} or HMGB-deficient *ssrp1a*$^{1-518}$, males and females hatched with fully developed heads and eyes, and proliferation and differentiation of eye-antennal imaginal discs proceeded normally (supplementary material Figs S5-S7 and Table S1). Strikingly, when *Drosophila Ssrp*^{RNAi} was co-expressed with zebrafish *ssrp1b*, *ssrp1a* or *ssrp1a*$^{1-518}$, the defects caused by *Ssrp* knockdown were substantially rescued (Fig. 4G-L″,P-R″; supplementary material Figs S6, S7). The majority of adult females and males hatched and displayed normal heads and eyes (supplementary material Table S1), apart from males rescued by *ssrp1b* and *ssrp1a*$^{1-518}$, which exhibited slightly rough eyes. Proliferation and R-cell differentiation in eye-antennal discs were indistinguishable from controls. Hence, zebrafish *ssrp1b*, *ssrp1a* and *ssrp1a*$^{1-518}$ can substitute for *Drosophila Ssrp*. By contrast, truncated *ssrp1a*^{s819} did not rescue *Drosophila* Ssrp knockdown phenotypes (Fig. 4M-O″; supplementary material Fig. S6H,H′ and Table S1), indicating that it is neither functional nor acts as a dominant-negative fragment. Importantly, these findings argue that in zebrafish, Ssrp1b could perform all Ssrp1 functions, but probably fails to replace zygotic Ssrp1a owing to low expression levels. Moreover, because Ssrp1a$^{1-518}$ can replace *Drosophila* Ssrp, our data indicate that the C-terminal HMGB-domain is dispensable *in vivo*. This is consistent with similar observations *in vitro* (Abe et al., 2011), and the fact that the yeast homologue Pob3 lacking an endogenous HMGB-domain interacts with the HMGB proteins Nhp6a and Nph6b (Wittmeyer et al., 1999). Also, other proteins can compensate for their function, as yeast lacking both factors are viable (Costigan et al., 1994). Likewise, Ssrp1a$^{1-518}$ could interact with other HMGB proteins to carry out FACT functions, as zebrafish and *Drosophila* genomes each contain at least four HMGB-containing polypeptides (Ragab et al., 2006) (Ensembl Zv9; http://www.ensembl.org/Danio_rerio/Info/Index). Our *in vivo* findings suggest that, despite the presence of an endogenous HMGB domain, *Drosophila*, and probably metazoans in general, have maintained the molecular components for Pob3-like FACT function. Hence, the basic mechanism of histone reorganisation between unicellular and multicellular organisms may be conserved independently of gene fusion/separation events associated with Ssrp1 evolution.

Ssrp1a has essential functions in basic cellular processes, including DNA synthesis and gene transcription. We propose that

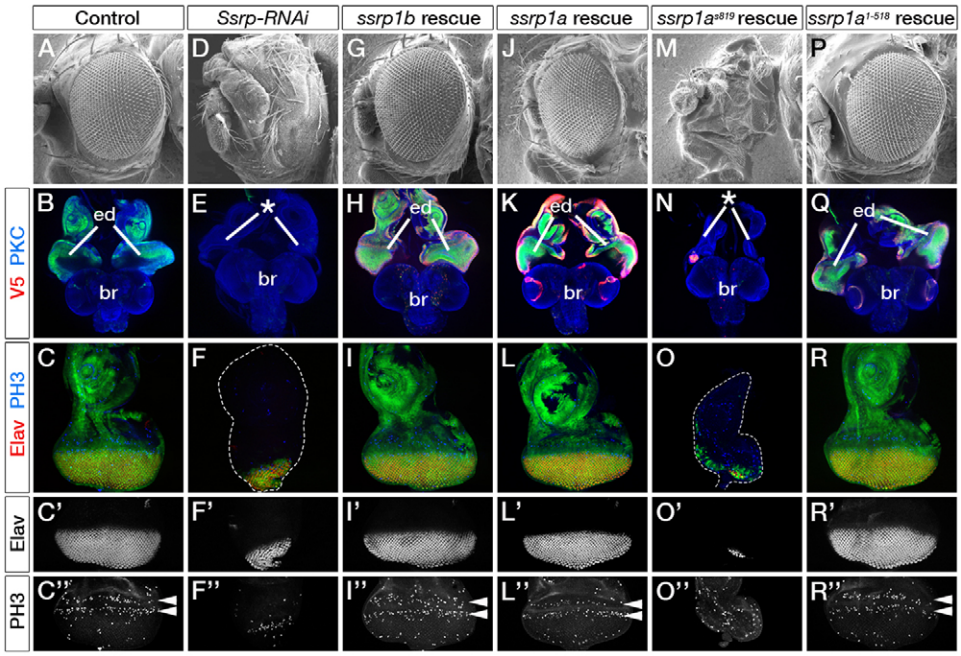

Fig. 4. *ssrp1b*, *ssrp1a* and *ssrp1a*$^{1-518}$ substitute *Drosophila Ssrp* function in the eye. (**A-R″**) For full genotypes and sample numbers, see supplementary material Table S1. (A,D,G,J,M,P) Scanning electron micrographs of leftward-facing adult female *Drosophila* heads. (B,E,H,K,N,Q) Confocal images of female third instar larval eye-antennal discs (ed) and brains (br) labelled with anti-PKC (blue). GFP signals indicate the areas of transgene expression, and V5 labelling (red) the presence of *Danio rerio* Ssrp1b-V5, Ssrp1a-V5, Ssrp1a^{s819}-V5 or Ssrp1a$^{1-518}$-V5. Anterior is up. (C-C″,F-F″,I-I″,L-L″,O-O″,R-R″) Eye-antennal discs and single channels of eye fields labelled with anti-Elav (red or white), visualising R-cell differentiation, and anti-PH3 (blue or white), monitoring two mitotic waves (arrowheads). (A-C″) Controls show adult eyes with a regular array of ommatidia and eye-imaginal discs with differentiated R-cells and two waves of dividing cells. (D-F″) *Drosophila* Ssrp knockdown causes the loss of adult eyes, and eye-antennal discs are significantly smaller (asterisk in E). (G-R″) *ssrp1b* (G-I″), *ssrp1a* (J-L″) and *ssrp1a*$^{1-518}$ (P-R″) expression rescues eye defects caused by *Ssrp*^{RNAi}. Expression of *ssrp1a*^{s819} (M-O″) fails to rescue. Asterisk in N indicates eye-antennal disc defects. (F,O) Dashed lines outline eye-antennal discs.

the spatiotemporal regulation of *ssrp1a* expression and the aforementioned functions are pivotal for achieving the appropriate rate of cell division and growth of each tissue, ensuring the correct shape, size and organ proportions in the developing embryo. Three lines of evidence indicate that maternal and zygotic Ssrp1a function in a specific rather than ubiquitous fashion in zebrafish embryogenesis. First, the onset of zygotic defects in *ssrp1a*^{s819} mutants is tissue specific. Phenotypes in the eye precede those in the liver but at the same stage no phenotypes are apparent in the somites, despite an earlier phase of extensive proliferation (Sugiyama et al., 2009), suggesting that these dynamics cannot be explained solely by protein turnover associated with replication. This is consistent with specific requirements for Ssrp1a in plant development (Lolas et al., 2010). Second, zygotic *ssrp1a*-expression domains are dynamic over time and often spatially restricted, including presumptive progenitor populations. This is in line with histone chaperones performing functions central to the properties of progenitor populations. Indeed, zebrafish with germ cells lacking maternal and zygotic Ssrp1a develop into sterile males, indicative of essential Ssrp1a functions in germ cell formation (K.K. and E.A.O., unpublished). Third, the developmental defects in *ssrp1a* mutants differ significantly in their timely appearance and severity from those in mutants carrying lesions in other genes performing similar fundamental cellular functions (Ryu et al., 2005).

In summary, our study uncovers essential functions of Ssrp1a in ensuring coordinated replication and RNA transcription in vertebrate embryos, underscoring the complex interplay between chromatin state and gene expression programmes during organ differentiation and growth.

Acknowledgements

We thank the NIMR aquatics team for fish care; D. Stainier, H. Field and P. Dong for joining forces for the Liver^{plus}Screen; and A. Miyawaki, A. Sakaue-Sawano, J. Fischer, T. Hawkins, G. Kassiotis, D. Wilkinson, the Bloomington *Drosophila* Stock Center and the DSHB (University of Iowa) for reagents or discussions.

Funding

This work was funded by the Medical Research Council [U117581329 to K.K., D.S. and E.A.O.; and U117581332 to H.A. and I.S.]. Deposited in PMC for release after 6 months.

Competing interests statement

The authors declare no competing financial interests.

Supplementary material

Supplementary material available online at
http://dev.biologists.org/lookup/suppl/doi:10.1242/dev.093583/-/DC1

References

Abe, T., Sugimura, K., Hosono, Y., Takami, Y., Akita, M., Yoshimura, A., Tada, S., Nakayama, T., Murofushi, H., Okumura, K. et al. (2011). The histone chaperone facilitates chromatin transcription (FACT) protein maintains normal replication fork rates. *J. Biol. Chem.* **286**, 30504-30512.

Bai, X., Kim, J., Yang, Z., Jurynec, M. J., Akie, T. E., Lee, J., LeBlanc, J., Sessa, A., Jiang, H., DiBiase, A. et al. (2010). TIF1gamma controls erythroid cell fate by regulating transcription elongation. *Cell* **142**, 133-143.

Belotserkovskaya, R., Oh, S., Bondarenko, V. A., Orphanides, G., Studitsky, V. M. and Reinberg, D. (2003). FACT facilitates transcription-dependent nucleosome alteration. *Science* **301**, 1090-1093.

Berghmans, S., Murphey, R. D., Wienholds, E., Neuberg, D., Kutok, J. L., Fletcher, C. D., Morris, J. P., Liu, T. X., Schulte-Merker, S., Kanki, J. P. et al. (2005). tp53 mutant zebrafish develop malignant peripheral nerve sheath tumors. *Proc. Natl. Acad. Sci. USA* **102**, 407-412.

Brewster, N. K., Johnston, G. C. and Singer, R. A. (2001). A bipartite yeast SSRP1 analog comprised of Pob3 and Nhp6 proteins modulates transcription. *Mol. Cell. Biol.* **21**, 3491-3502.

Cao, S., Bendall, H., Hicks, G. G., Nashabi, A., Sakano, H., Shinkai, Y., Gariglio, M., Oltz, E. M. and Ruley, H. E. (2003). The high-mobility-group box protein SSRP1/T160 is essential for cell viability in day 3.5 mouse embryos. *Mol. Cell. Biol.* **23**, 5301-5307.

Chen, J., Ruan, H., Ng, S. M., Gao, C., Soo, H. M., Wu, W., Zhang, Z., Wen, Z., Lane, D. P. and Peng, J. (2005). Loss of function of def selectively up-regulates Delta113p53 expression to arrest expansion growth of digestive organs in zebrafish. *Genes Dev.* **19**, 2900-2911.

Cheyette, B. N., Green, P. J., Martin, K., Garren, H., Hartenstein, V. and Zipursky, S. L. (1994). The Drosophila sine oculis locus encodes a homeodomain-containing protein required for the development of the entire visual system. *Neuron* **12**, 977-996.

Costigan, C., Kolodrubetz, D. and Snyder, M. (1994). NHP6A and NHP6B, which encode HMG1-like proteins, are candidates for downstream components of the yeast SLT2 mitogen-activated protein kinase pathway. *Mol. Cell. Biol.* **14**, 2391-2403.

Field, H. A., Ober, E. A., Roeser, T. and Stainier, D. Y. (2003). Formation of the digestive system in zebrafish. I. Liver morphogenesis. *Dev. Biol.* **253**, 279-290.

Formosa, T. (2008). FACT and the reorganized nucleosome. *Mol. Biosyst.* **4**, 1085-1093.

Formosa, T., Eriksson, P., Wittmeyer, J., Ginn, J., Yu, Y. and Stillman, D. J. (2001). Spt16-Pob3 and the HMG protein Nhp6 combine to form the nucleosome-binding factor SPN. *EMBO J.* **20**, 3506-3517.

Gambus, A., Jones, R. C., Sanchez-Diaz, A., Kanemaki, M., van Deursen, F., Edmondson, R. D. and Labib, K. (2006). GINS maintains association of Cdc45 with MCM in replisome progression complexes at eukaryotic DNA replication forks. *Nat. Cell Biol.* **8**, 358-366.

Geisler, R. (2002). Mapping and cloning. In *Zebrafish: A Practical Approach* (ed. C. Nusslein-Volhard and R. Dahm), pp. 175-212. Oxford: Oxford University Press.

Hadjieconomou, D., Rotkopf, S., Alexandre, C., Bell, D. M., Dickson, B. J. and Salecker, I. (2011). Flybow: genetic multicolor cell labeling for neural circuit analysis in Drosophila melanogaster. *Nat. Methods* **8**, 260-266.

Jao, C. Y. and Salic, A. (2008). Exploring RNA transcription and turnover in vivo by using click chemistry. *Proc. Natl. Acad. Sci. USA* **105**, 15779-15784.

Keller, D. M. and Lu, H. (2002). p53 serine 392 phosphorylation increases after UV through induction of the assembly of the CK2.hSPT16.SSRP1 complex. *J. Biol. Chem.* **277**, 50206-50213.

Keller, D. M., Zeng, X., Wang, Y., Zhang, Q. H., Kapoor, M., Shu, H., Goodman, R., Lozano, G., Zhao, Y. and Lu, H. (2001). A DNA damage-induced p53 serine 392 kinase complex contains CK2, hSpt16, and SSRP1. *Mol. Cell* **7**, 283-292.

Korzh, S., Emelyanov, A. and Korzh, V. (2001). Developmental analysis of ceruloplasmin gene and liver formation in zebrafish. *Mech. Dev.* **103**, 137-139.

Leung, A. Y., Leung, J. C., Chan, L. Y., Ma, E. S., Kwan, T. T., Lai, K. N., Meng, A. and Liang, R. (2005). Proliferating cell nuclear antigen (PCNA) as a proliferative marker during embryonic and adult zebrafish hematopoiesis. *Histochem. Cell Biol.* **124**, 105-111.

Li, Y., Zeng, S. X., Landais, I. and Lu, H. (2007). Human SSRP1 has Spt16-dependent and -independent roles in gene transcription. *J. Biol. Chem.* **282**, 6936-6945.

Lin, J. W., Biankin, A. V., Horb, M. E., Ghosh, B., Prasad, N. B., Yee, N. S., Pack, M. A. and Leach, S. D. (2004). Differential requirement for ptf1a in endocrine and exocrine lineages of developing zebrafish pancreas. *Dev. Biol.* **270**, 474-486.

Lolas, I. B., Himanen, K., Gronlund, J. T., Lynggaard, C., Houben, A., Melzer, M., Van Lijsebettens, M. and Grasser, K. D. (2010). The transcript elongation factor FACT affects Arabidopsis vegetative and reproductive development and genetically interacts with HUB1/2. *Plant J.* **61**, 686-697.

Malone, E. A., Clark, C. D., Chiang, A. and Winston, F. (1991). Mutations in SPT16/CDC68 suppress cis- and trans-acting mutations that affect promoter function in Saccharomyces cerevisiae. *Mol. Cell. Biol.* **11**, 5710-5717.

Masai, I., Stemple, D. L., Okamoto, H. and Wilson, S. W. (2000). Midline signals regulate retinal neurogenesis in zebrafish. *Neuron* **27**, 251-263.

Morillo-Huesca, M., Maya, D., Muñoz-Centeno, M. C., Singh, R. K., Oreal, V., Reddy, G. U., Liang, D., Géli, V., Gunjan, A. and Chávez, S. (2010). FACT prevents the accumulation of free histones evicted from transcribed chromatin and a subsequent cell cycle delay in G1. *PLoS Genet.* **6**, e1000964.

Noël, E. S., Casal-Sueiro, A., Busch-Nentwich, E., Verkade, H., Dong, P. D., Stemple, D. L. and Ober, E. A. (2008). Organ-specific requirements for Hdac1 in liver and pancreas formation. *Dev. Biol.* **322**, 237-250.

Noël, E. S., Reis, M. D., Arain, Z. and Ober, E. A. (2010). Analysis of the Albumin/alpha-Fetoprotein/Afamin/Group specific component gene family in the context of zebrafish liver differentiation. *Gene Expr. Patterns* **10**, 237-243.

Ober, E. A., Verkade, H., Field, H. A. and Stainier, D. Y. (2006). Mesodermal Wnt2b signalling positively regulates liver specification. *Nature* **442**, 688-691.

Odenthal, J. and Nüsslein-Volhard, C. (1998). fork head domain genes in zebrafish. *Dev. Genes Evol.* **208**, 245-258.

Ohtani, K., DeGregori, J. and Nevins, J. R. (1995). Regulation of the cyclin E gene by transcription factor E2F1. *Proc. Natl. Acad. Sci. USA* **92**, 12146-12150.

Orphanides, G., Wu, W. H., Lane, W. S., Hampsey, M. and Reinberg, D. (1999). The chromatin-specific transcription elongation factor FACT comprises human SPT16 and SSRP1 proteins. *Nature* **400**, 284-288.

Ragab, A., Thompson, E. C. and Travers, A. A. (2006). High mobility group proteins HMGD and HMGZ interact genetically with the Brahma chromatin remodeling complex in Drosophila. *Genetics* **172**, 1069-1078.
Ransom, M., Dennehey, B. K. and Tyler, J. K. (2010). Chaperoning histones during DNA replication and repair. *Cell* **140**, 183-195.
Ryu, S., Holzschuh, J., Erhardt, S., Ettl, A. K. and Driever, W. (2005). Depletion of minichromosome maintenance protein 5 in the zebrafish retina causes cell-cycle defect and apoptosis. *Proc. Natl. Acad. Sci. USA* **102**, 18467-18472.
Saunders, A., Werner, J., Andrulis, E. D., Nakayama, T., Hirose, S., Reinberg, D. and Lis, J. T. (2003). Tracking FACT and the RNA polymerase II elongation complex through chromatin in vivo. *Science* **301**, 1094-1096.
Shimojima, T., Okada, M., Nakayama, T., Ueda, H., Okawa, K., Iwamatsu, A., Handa, H. and Hirose, S. (2003). Drosophila FACT contributes to Hox gene expression through physical and functional interactions with GAGA factor. *Genes Dev.* **17**, 1605-1616.
Shkumatava, A., Fischer, S., Müller, F., Strahle, U. and Neumann, C. J. (2004). Sonic hedgehog, secreted by amacrine cells, acts as a short-range signal to direct differentiation and lamination in the zebrafish retina. *Development* **131**, 3849-3858.
Stillman, D. J. (2010). Nhp6: a small but powerful effector of chromatin structure in Saccharomyces cerevisiae. *Biochim. Biophys. Acta* **1799**, 175-180.
Sugiyama, M., Sakaue-Sawano, A., Iimura, T., Fukami, K., Kitaguchi, T., Kawakami, K., Okamoto, H., Higashijima, S. I. and Miyawaki, A. (2009). Illuminating cell-cycle progression in the developing zebrafish embryo. *Proc. Natl. Acad. Sci. USA* **106**, 20812-20817.
Tan, B. C., Chien, C. T., Hirose, S. and Lee, S. C. (2006). Functional cooperation between FACT and MCM helicase facilitates initiation of chromatin DNA replication. *EMBO J.* **25**, 3975-3985.
Vogelstein, B., Lane, D. and Levine, A. J. (2000). Surfing the p53 network. *Nature* **408**, 307-310.
Westerfield, M. (2000). *The Zebrafish Book. A Guide for the Laboratory Use of Zebrafish (Danio rerio)*. Eugene, OR: University of Oregon Press.
Winkler, D. D. and Luger, K. (2011). The histone chaperone FACT: structural insights and mechanisms for nucleosome reorganization. *J. Biol. Chem.* **286**, 18369-18374.
Wittmeyer, J., Joss, L. and Formosa, T. (1999). Spt16 and Pob3 of Saccharomyces cerevisiae form an essential, abundant heterodimer that is nuclear, chromatin-associated, and copurifies with DNA polymerase alpha. *Biochemistry* **38**, 8961-8971.
Yamaguchi, T., Cubizolles, F., Zhang, Y., Reichert, N., Kohler, H., Seiser, C. and Matthias, P. (2010). Histone deacetylases 1 and 2 act in concert to promote the G1-to-S progression. *Genes Dev.* **24**, 455-469.

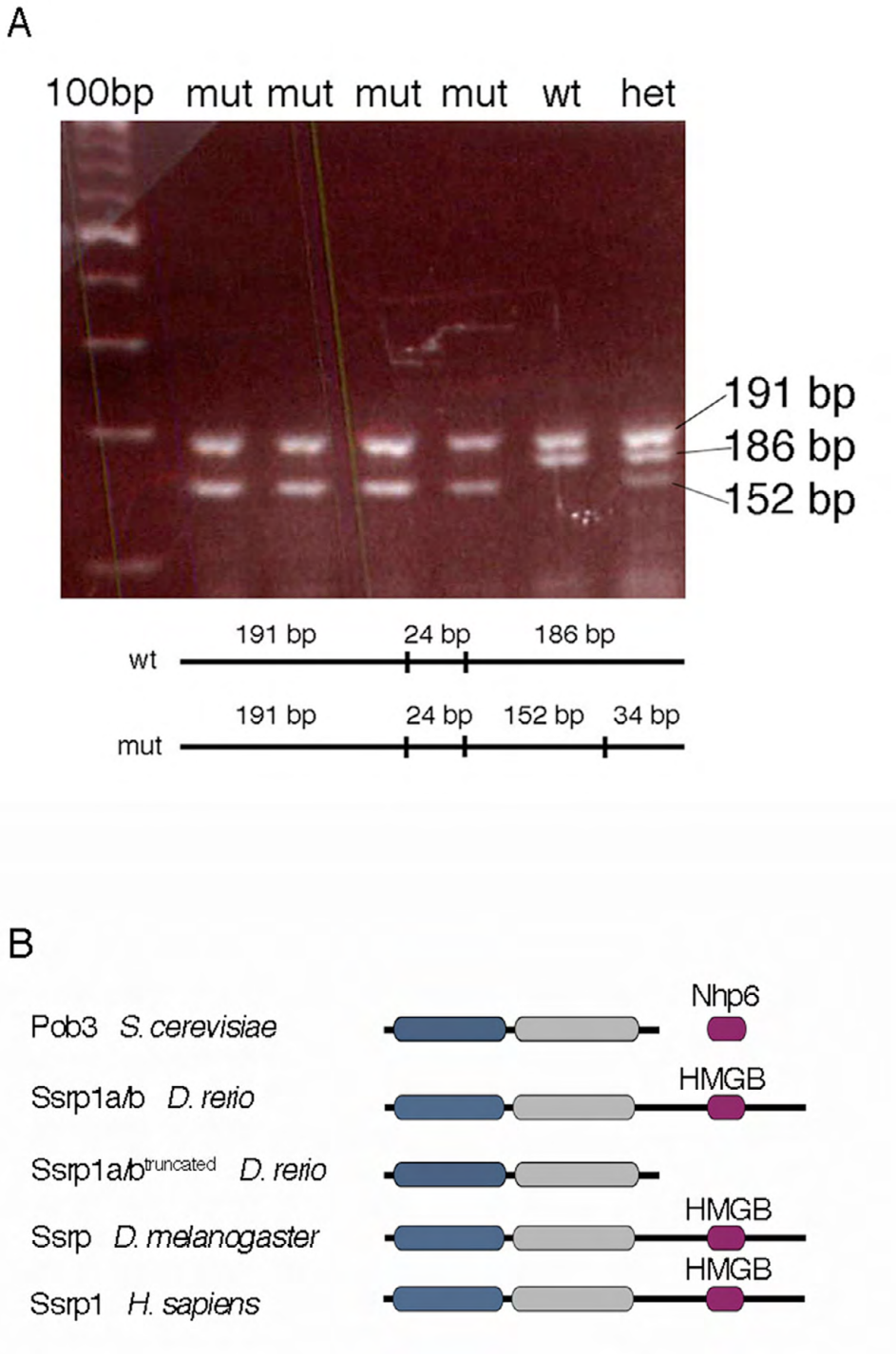

Fig. S1. *ssrp1a*^{s819} genotyping and Ssrp1 protein structure through evolution. (**A**) For genotyping of *cmp*^{s819} embryos, a dCaps assay was generated creating a *Hin*fI restriction site including the *ssrp1a*^{s819} mutation. PCR amplification and subsequent *Hin*fI digest from homozygous mutant, wild-type and heterozygous embryos confirmed the identified lesion. (**B**) Comparison of zebrafish Ssrp1a and Ssrp1b with other Ssrp1 homologues. Short forms of zebrafish Ssrp1a and Ssrp1b lacking the HMGB domain characteristic for metazoan Ssrp1 are predicted by EST-evidence (NCBI, Ensembl_Zv9).

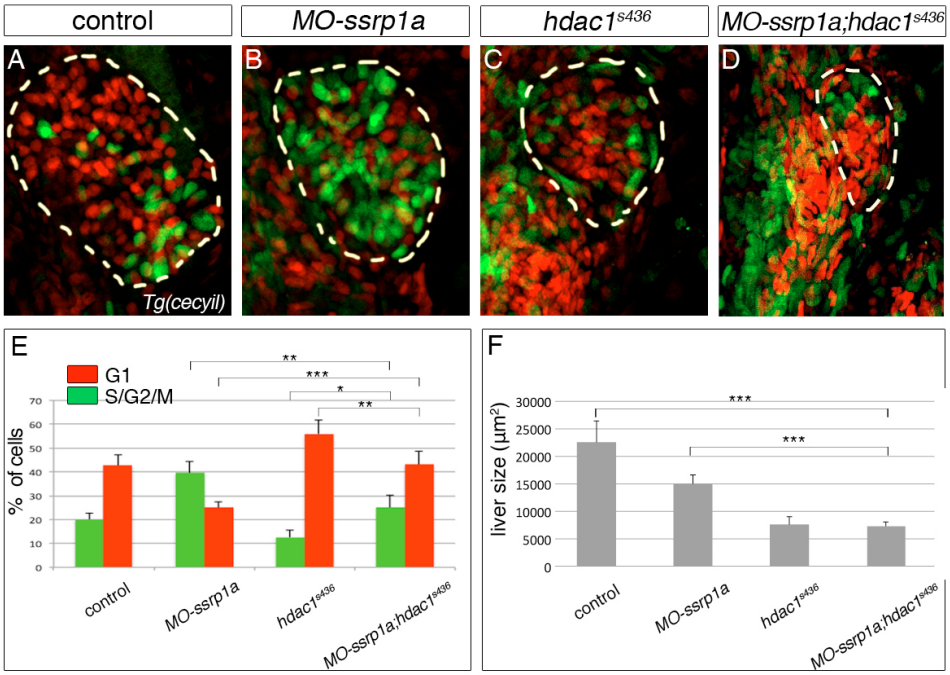

Fig. S2. Ssrp1a and Hdac1 are required in different phases of the cell cycle. (**A-D**) Transgenic *cecyil* expression marks the cell cycle dynamics in the liver (outlined in yellow; ventral views). Cells in G_1 phase are in red and cells in $S/G_2/M$ phase in green. (**E**) Quantification of both populations in *MO-ssrp1a* and *hdac1*^{s436} reveal significant changes compared with controls (G_1: *MO-ssrp1a*, $P<0.001$, *hdac1*^{s436}, $P<0.001$; $S/G_2/M$: *MO-ssrp1a*, $P<0.001$, *hdac1*^{s436}, $P<0.05$). Enrichment of *MO-ssrp1a* cells in $S/G_2/M$ phase indicate DNA replication defects, whereas enrichment of Hdac1-deficient cells in G_1 phase suggest impaired cell cycle progression. *MO-ssrp1a;hdac1*^{s436} embryos show a partial rescue of both populations compared with the individual loss-of-function phenotypes. (**F**) By contrast, liver size does not improve in *MO-ssrp1a;hdac1*^{s436} embryos compared with *MO-ssrp1a*, *hdac1*^{s436} and control (F). $*P<0.05$, $**P<0.01$, $***P<0.001$, determined by Student's *t*-test. Error bars represent s.e.m.

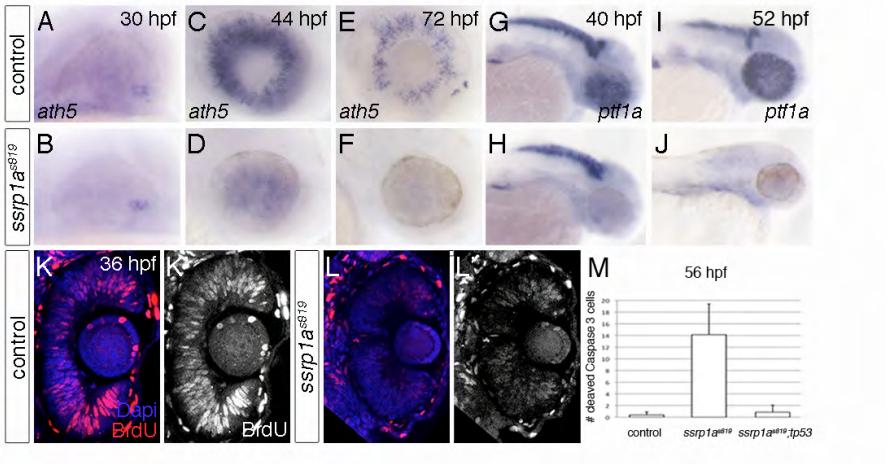

Fig. S3. Ssrp1a promotes differentiation and proliferation of the zebrafish eye. (**A-F**) Retinal *ath5* expression in *ssrp1a*^{s819} mutants is indistinguishable from controls at 30 hpf (A,B), but severely reduced at later stages (C-F). Lateral views, anterior to the right. (**K-L'**) BrdU incorporation in the eye is severely compromised in mutants compared to wild-type. Coronal sections with anterior to the top. (**G-J**) *ptf1a* in differentiating amacrine cells fails to be expressed in *ssrp1a*^{s819} mutants compared with controls at 40 hpf, whereas expression in the exocrine pancreas and CNS is indistinguishable (G,H). At 52 hpf, *ptf1a* expression is not detectable in any tissue of *ssrp1a*^{s819} mutants (I,J). Lateral views, anterior to the right. (**M**) Genetic depletion of Tp53 significantly rescues cell death in Ssrp1a-deficient cells in the eye. Error bars represent s.d.

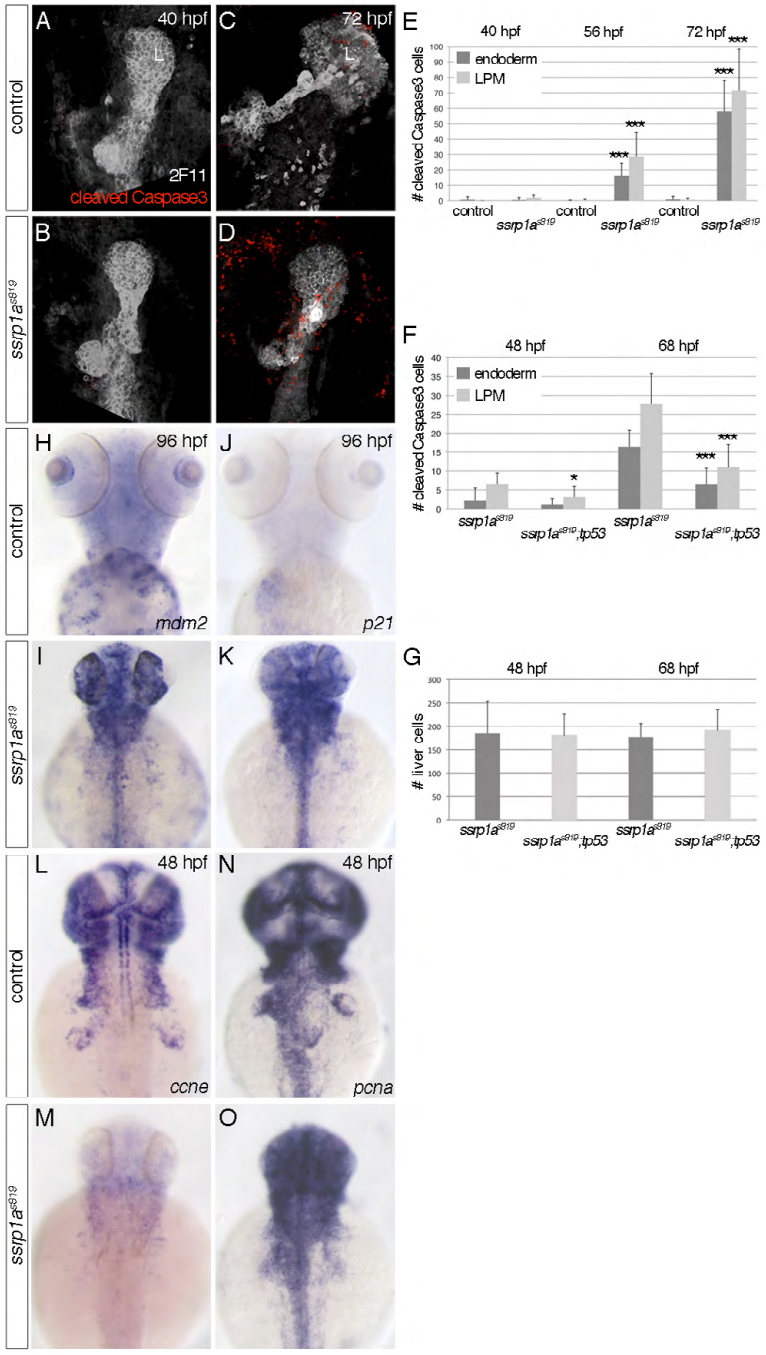

Fig. S4. Ssrp1a is required for cell survival. (**A-F**) Anti-cleaved Caspase-3 staining shows apoptosis in *ssrp1a*^{s819} mutant livers, co-stained with anti-2F11. Wild-type show no significant apoptosis during liver formation (A,B,E), whereas dying cells are found in *ssrp1a*^{s819} mutant endoderm and adjacent LPM starting around 48 hpf, and their number is significantly increased from 56 hpf (E). Loss of Tp53 partially rescues apoptosis in *ssrp1a*^{s819} mutant livers and LPM (F). This indicates that in addition other cell death mechanisms are activated in Ssrp1a-deficient cells. Notably, this rescue is less efficient than in the forming eye (supplementary material Fig. S3M), suggesting tissue-specific responses. (**G**) Importantly, the overall number of liver cells is not altered in the *ssrp1a*^{s819}*;tp53* mutants compared to *ssrp1a*^{s819} embryos at 48 and 68 hpf. (**H-K**) At 96 hpf, the expression of Tp53 target genes *mdm2* and *p21* is strongly increased in *ssrp1a*^{s819} mutants compared with controls. (**L-O**) Expression of *ccne* is already at 48 hpf severely reduced in *ssrp1a*^{s819} mutants (M), whereas *pcna* levels are not significantly altered (O). A-D are confocal projections of ventral views, H-O are dorsal views; all anterior to the top. **P*<0.05; ****P*<0.0005, determined by unpaired Student's *t*-test. Error bars represent s.d.

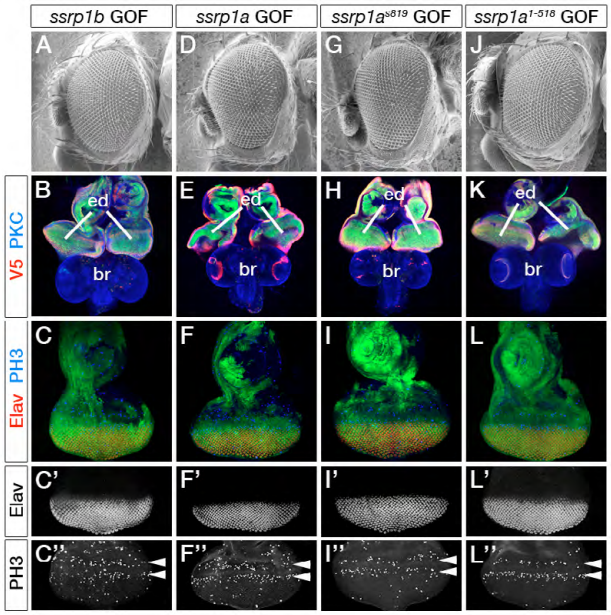

Fig. S5. Ectopic expression of *D. rerio ssrp1b*, *ssrp1a*, *ssrp1a^{s819}* and *ssrp1a$^{1-518}$* does not affect *Drosophila* eye development. (**A-L″**) Ectopic, (GOF) -of-function expression of *D. rerio ssrp1b* (A-C″), *ssrp1a* (D-F″), *ssrp1a^{s189}* (G-I″) or *ssrp1a$^{1-518}$* (J-L″) does not affect wild-type *Drosophila* eye development (c.f. Fig. 4A-C″). Full genotypes and sample numbers are provided in supplementary material Table S1. (A,D,G,J) Scanning electron micrographs of adult female *Drosophila* heads. Anterior is left. (B,E,H,K) Confocal images of female third instar larval eye-antennal discs (ed) and brains (br) labelled with anti-PKC (blue). GFP shows the area of transgene expression, and V5 labelling (red) the presence of *D. rerio* Ssrp1b-V5, Ssrp1a-V5, Ssrp1a^{s819}-V5 or Ssrp1a$^{1-518}$-V5. Anterior is up. (C-C″,F-F″,I-I″L-L″) Eye-antennal discs and single channel images of eye fields labelled with anti-Elav (red or white), visualizing R-cell differentiation, and anti-PH3 (blue or white), monitoring proliferation within two mitotic waves (arrowheads).

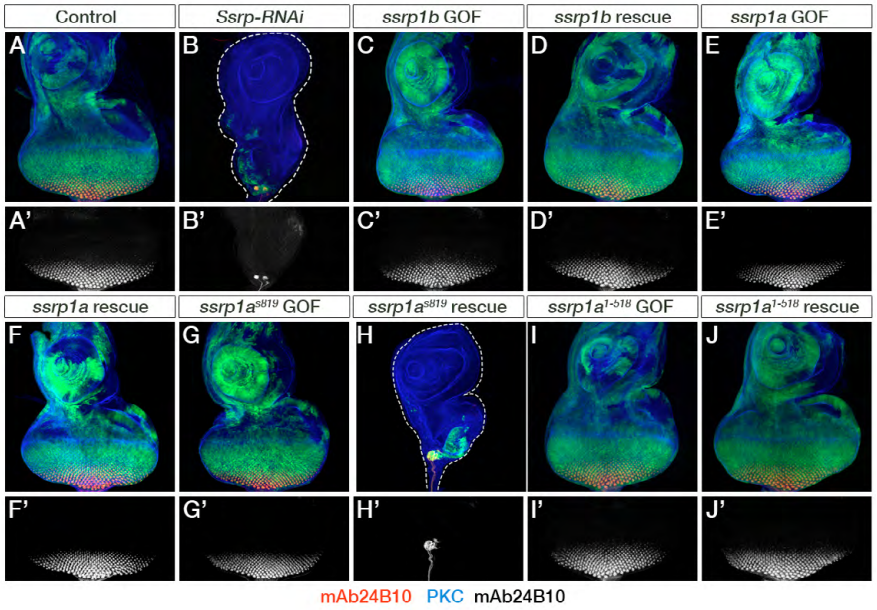

Fig. S6. *D. rerio ssrp1b*, *ssrp1a* and *ssrp1a$^{1-518}$* substitute *Drosophila Ssrp* function in the eye-antennal imaginal disc. Full genotypes and sample numbers are provided in supplementary material Table S1. (**A-J′**) Confocal images of female *Drosophila* eye-antennal imaginal discs. Green fluorescent protein signals indicate the areas of transgene expression. Anterior is up. Photoreceptor (R-cell) differentiation in the eye field is assessed by mAb24B10 labeling (red or white), anti-PKC is shown in blue. In wild type, R-cell differentiation proceeds normally (A,A′). Few *Ssrp^{RNAi}*-expressing cells differentiate into R-cells labeled with mAb24B10 (B,B′). Ectopic gain-of-function (GOF) expression of zebrafish *ssrp1b* (C,C′), *ssrp1a* (E,E′), *ssrp1a^{s819}* (G,G′) or *ssrp1a$^{1-518}$* (I,I′) does not affect R-cell differentiation. Expression of *Ssrp^{RNAi}* and *ssrp1b* (D,D′), *ssrp1a* (F,F′) or *ssrp1a$^{1-518}$* (J,J′) results in normal R-cell differentiation, whereas *ssrp1a^{s819}* expression is unable to rescue *Ssrp^{RNAi}* R-cell differentiation defects (H,H′). Dashed lines outline eye-antennal discs in B and H.

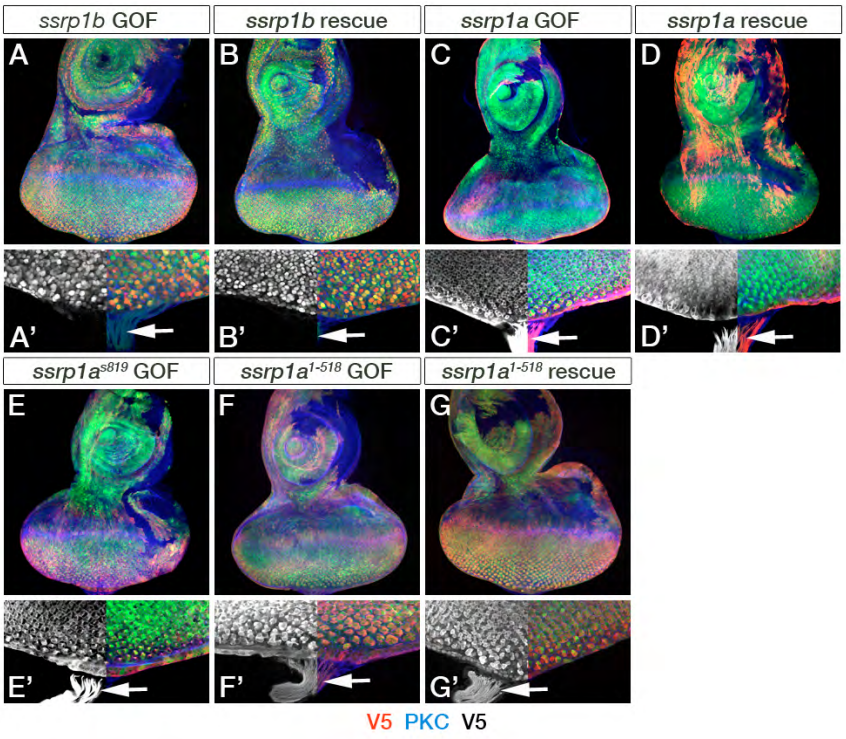

Fig. S7. Nuclear localisation of ectopic *D. rerio* Ssrp1 proteins in *Drosophila* eye-antennal imaginal discs. Full genotypes and sample numbers are provided in supplementary material Table S1. (**A-G'**) Confocal images of female third instar larval eye-antennal imaginal discs. GFP signals indicate the area of transgene expression, anti-PKC is shown in blue and anti-V5 in red. Anterior is up. A'-G' show higher magnification images of the posterior eye field. In the left half of panels, V5 labelling is shown in white. R-cell axons exit the eye disc and project through the optic stalk (arrow). V5 labelling reveals nuclear localisation of ectopic Ssrp1b-V5 in gain-of-function (GOF; A) and rescue experiments (B). In addition to nuclear localisation, Ssrp1a-V5, Ssrp1a^{s819}-V5 and Ssrp1a$^{1-518}$-V5 are expressed in the cytoplasm in gain-of-function (GOF; C,E,F) and rescue experiments (D,G), as revealed by V5 labelling of R-cell axons.

Table S1. Genotypes and quantifications of gene deletion/replacement experiments in *Drosophila*

	Genotype	Adult hatching rates % (*n*=)	Panel	SEM/Staining	*n*=
Control	*ey$^{3.5}$-FLP/+; act>y^{+}>Gal4 UAS-GFP/CyO; UAS-Dcr2/+*		4A	SEM	15
			4B	V5/PKC	25
			4C-C″	Elav/PH3	18
			S6A,A′	mAb24B10/PKC	8
***Ssrp*-RNAi**	*ey$^{3.5}$-FLP/+; act>y^{+}>Gal4 UAS-GFP/+; UAS-Dcr2/UAS-Ssrp^{RNAi}*	♂: 0% (232) ♀: 5.5% (146) with partial heads	4D	SEM	14
			4E	V5/PKC	29
			4F-F″	Elav/PH3	7
			S6B,B′	mAb24B10/PKC	7
***ssrp1b* GOF**	*ey$^{3.5}$-FLP/+; act>y^{+}>Gal4 UAS-GFP/UAS-ssrp1b-V5; UAS-Dcr2/+*	♂: 100% (136) ♀: 100% (113)	S5A	SEM	21
			S5B, S7A,A′	V5/PKC	9
			S5C-C″	Elav/PH3	19
			S6C,C′	mAb24B10/PKC	8
***ssrp1b* rescue**	*ey$^{3.5}$-FLP/+; act>y^{+}>Gal4 UAS-GFP/UAS-ssrp1b-V5; UAS-Dcr2/UAS-Ssrp^{RNAi}*	♂: 96.7% (300) ♀: 100% (322)	4G	SEM	21
			4H, S7B,B′	V5/PKC	9
			4I-I″	Elav/PH3	10
			S6D,D′	mAb24B10/PKC	9
***ssrp1a* GOF**	*ey$^{3.5}$-FLP/+; act>y^{+}>Gal4 UAS-GFP/UAS-ssrp1a-V5; UAS-Dcr2/+*	♂: 100% (191) ♀: 100% (188)	S5D	SEM	8
			S5E, S7C,C′	V5/PKC	28
			S5F-F″	Elav/PH3	4
			S6E, E′	mAb24B10/PKC	12
***ssrp1a* rescue**	*ey$^{3.5}$-FLP/+; act>y^{+}>Gal4 UAS-GFP/UAS-ssrp1a-V5; UAS-Dcr2/UAS-Ssrp^{RNAi}*	♂: 100% (246) ♀: 100% (229)	4J	SEM	9
			4K, S7D,D′	V5/PKC	18
			4L-L″	Elav/PH3	18
			S6F,F′	mAb24B10/PKC	8
***ssrp1a^{s819}* GOF**	*ey$^{3.5}$-FLP/+; act>y^{+}>Gal4 UAS-GFP/UAS-ssrp1a^{s819}-V5; UAS-Dcr2/+*	♂: 100% (105) ♀: 100% (126)	S5G	SEM	5
			S5H, S7E,E′	V5/PKC	18
			S5I-I″	Elav/PH3	13
			S6G,G′	mAb24B10/PKC	9
***ssrp1a^{s819}* rescue**	*ey$^{3.5}$-FLP/+; act>y^{+}>Gal4 UAS-GFP/UAS-ssrp1a^{s819}-V5; UAS-Dcr2/UAS-Ssrp^{RNAi}*	♂: 0% (163) ♀: 4% (151) with partial heads	4M	SEM	5
			4N	V5/PKC	10
			4O-O″	Elav/PH3	4
			S6H,H′	mAb24B10/PKC	8
***ssrp1a$^{1-518}$* GOF**	*ey$^{3.5}$-FLP/+; act>y^{+}>Gal4 UAS-GFP/UAS-ssrp1a$^{1-518}$-V5; UAS-Dcr2/+*	♂: 100% (114) ♀: 100% (105)	S5J	SEM	6
			S5K, S7F,F′	V5/PKC	12
			S5L-L″	Elav/PH3	16
			S6I,I′	mAb24B10/PKC	15
***ssrp1a$^{1-518}$* rescue**	*ey$^{3.5}$-FLP/+; act>y^{+}>Gal4 UAS-GFP/UAS-ssrp1a$^{1-518}$-V5; UAS-Dcr2/UAS-Ssrp^{RNAi}*	♂: 97.3% (187) ♀: 100% (175)	4P	SEM	28
			4Q, S7G,G′	V5/PKC	38
			4R-R″	Elav/PH3	21
			S6J,J′	mAb24B10/PKC	13

SEM, scanning electron microscopy

Table S2. *Drosophila* genetic crosses

Experiment	Driver stock	Crossed to*
***Drosophila Ssrp*-RNAi**	*ey$^{3.5}$-FLP; act>y^{+}>Gal4 UAS-GFP/CyO; UAS-Dcr2*	*UAS-Ssrp^{RNAi}* (*P{TRiP.JF02120}attP2*)
***ssrp1b, ssrp1a, ssrp1a^{s819}* and *ssrp1a$^{1-518}$* gain-of-function**	*ey$^{3.5}$-FLP; act>y^{+}>Gal4 UAS-GFP/CyO; UAS-Dcr2*	*UAS-ssrp1b-V5* *UAS-ssrp1a-V5* *UAS-ssrp1a^{s819}-V5* *UAS-ssrp1a$^{1-518}$-V5*
***ssrp1b, ssrp1a, ssrp1a^{s819}* and *ssrp1a$^{1-518}$* cross-species rescue**	*ey$^{3.5}$-FLP; act>y^{+}>Gal4 UAS-GFP/CyO; UAS-Dcr2*	*UAS-ssrp1b-V5; UAS-Ssrp^{RNAi}* *UAS-ssrp1a-V5; UAS-Ssrp^{RNAi}* *UAS-ssrp1a^{s819}-V5; UAS-Ssrp^{RNAi}* *UAS-ssrp1a$^{1-518}$-V5; UAS-Ssrp^{RNAi}*

*****Crosses were maintained at 25°C on standard medium. *ey$^{3.5}$-FLP/+;act>y^{+}>Gal4 UAS-GFP/CyO; UAS-Dcr2/+* served as controls.